HETEROCYCLES, Vol. 106, No. 4, 2023, pp. 707 - 715. © 2023 The Japan Institute of Heterocyclic Chemistry
Received, 27th January, 2023, Accepted, 20th February, 2023, Published online, 6th March, 2023
DOI: 10.3987/COM-23-14814

CHEMICAL STRUCTURES AND CELL DEATH INDUCING ACTIVITIES OF THE METABOLITES OF *ASPERGILLUS TERREUS*

Takahiro Matsumoto,* Masaya Okayama, Hayato Yoshikawa, Shifu Maeda, Takahiro Kitagawa, and Tetsushi Watanabe*

Department of Public Health, Kyoto Pharmaceutical University, Misasagi, Yamashina-Ku, Kyoto 607-8412, Japan; E-mail: tmatsumo@mb.kyoto-phu.ac.jp (T.M.), watanabe@mb.kyoto-phu.ac.jp (T.W.)

Abstract – A new steroid, terreus steroid (**1**), and eight known compounds (**2**–**9**) have been isolated from the airborne-derived fungus *Aspergillus terreus*. The structure of terreus steroid (**1**) was elucidated based on the chemical/physicochemical evidence. The cell death-inducing activities of the isolated compounds with or without Adriamycin (ADR) were observed using time-lapse cell imaging. Among the isolated compounds, terreus steroid (**1**) and territrem B (**3**) significantly reduced the number of mitotic entry cells at 60 μM. In addition, terreus steroid (**1**), territrem C (**2**), territrem B (**3**), *epi*-aszonalenin A (**5**), and methyl 3,4,5-trimethoxy-2-(2-(nicotinamido)benzamido)benzoate (**6**) significantly increased the number of dead cells on Adriamycin-treated HeLa cells.

The fungus *Aspergillus terreus* is commonly found in various habitats including the soil of the river,[1] the soil of the mountain,[2] the tissue of coral,[3] and the tissue of plants.[4] In addition, *A. terreus* have been reported as the rich source of several bioactive compounds. For example, α-glucosidase inhibitory butanolide analogues,[5] cytotoxic alkaloids,[6] nitric oxide production inhibitory dihydrobenzofuran derivatives,[7] and β-site amyloid precursor protein-cleaving enzyme 1 inhibitory meroterpenoids[1] have been reported as the secondary metabolites of *A. terreus*. On our ongoing research program for the discovery of new cancer treatment agents, we previously reported the Wnt signal inhibitor from *Lindera umbellate*,[8] the anti-proliferative agents against cancer stem cells from *Petasites japonicus*,[9] and the heat shock protein (HSP) expression inhibitors from *Hypericum erectum*.[10] Especially, HSP expression inhibitors enhanced the cell death inducing activity of Adriamycin (ADR) via inhibitory effects against

anti-apoptotic effects of HSP. Continuously, we started the isolation of several bioactive compounds produced by *A. terreus* to find the enhancers of cancer treatment agents such as ADR.

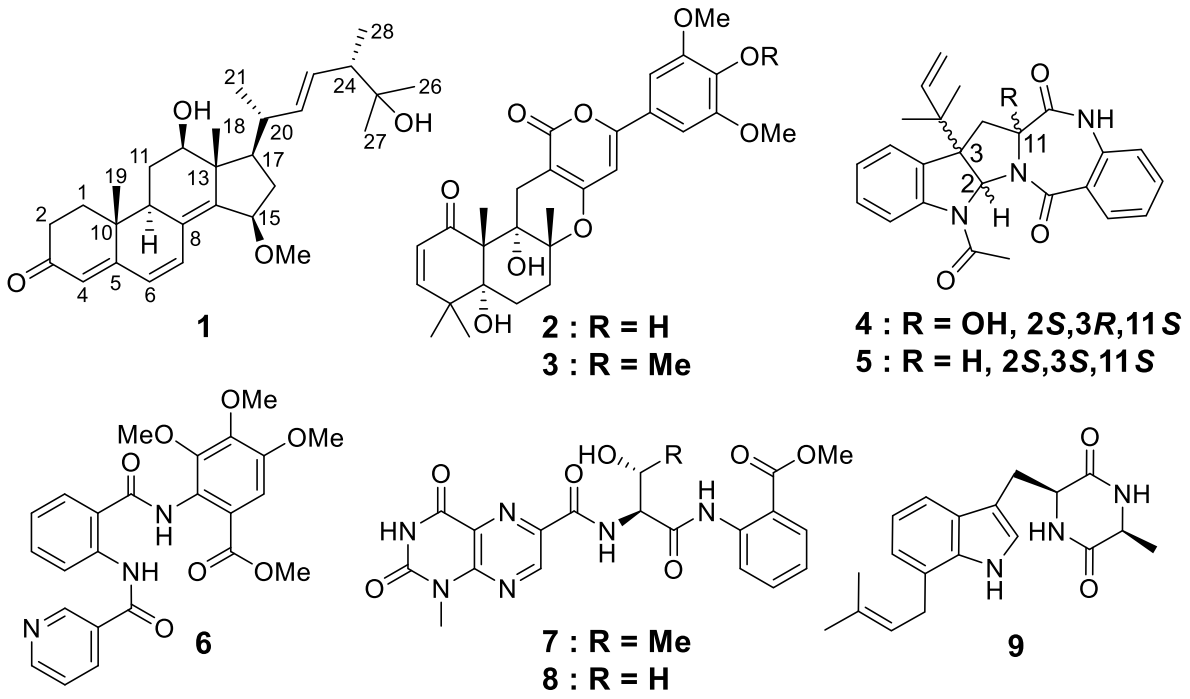

Figure 1. The chemical structures of the isolated compounds produced by *A. terreus*

The fungus, *A. terreus* JKYM-KI3 obtained from airborne of Kyoto was cultured in a potato dextrose agar (PDA). The EtOAc soluble fraction was obtained after incubation of the culture at 27 °C for 20 days. The EtOAc soluble fraction was purified by normal and reversed phase silica gel column chromatography followed by HPLC to give a new steroid: terreus steroid (**1**) together with eight known compounds, territrem C (**2**),[11] territrem B (**3**),[12] asterrelenin (**4**),[13] *epi*-aszonalenin A (**5**),[14] and methyl 3,4,5-trimethoxy-2-(2-(nicotinamido)benzamido)benzoate (**6**),[15] terrelumamides A (**7**),[16] terrelumamides B (**8**),[16] terezine D (**9**) (Figure 1).[17]

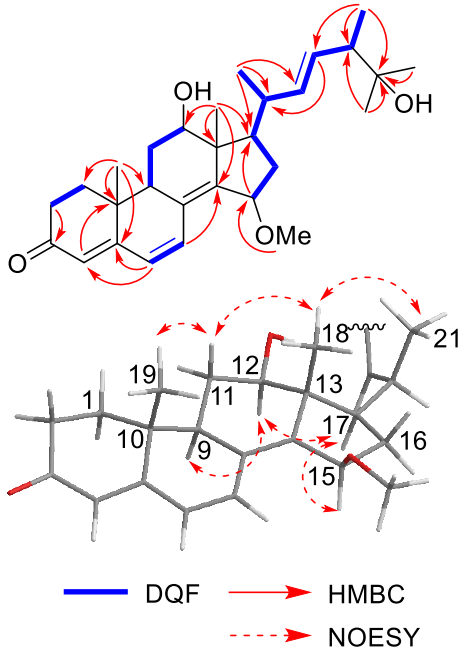

Figure 2. The important 2D-NMR correlations of terreus steroid (**1**)

Terreus steroid (**1**) was obtained as a colorless amorphous powder with positive optical rotation ($[a]^{25}_{D}$ +201.9 in methanol). The molecular formula ($C_{29}H_{42}O_4$) was determined via high-resolution fast atom bombardment mass spectrometry (HRFABMS) and ^{13}C NMR spectroscopy. The ^{1}H and ^{13}C NMR spectra (chloroform-*d*) of **1** (Table 1) showed characteristic signals of ergosterol derivative that have ordinal 6/6/6/5 ring system {two methyl groups [δ_H 1.04 (s, H-19) and 0.93 (s, H-18)], four methylene groups [δ_C 34.0 (C-1), 33.9 (C-2), 28.6 (C-11), and 29.6 (C-16)], two methine groups [δ_H 2.49 (m, H-9) and 1.82 (m, H-17)], two methine groups with oxygen function group [δ_H 3.76 (dd, J = 4.2, 11.4, H-12) and 4.44 (d-like, J = 3.6, H-15)], two quaternary carbons [δ_C 36.8 (C-10) and 48.9 (C-13)], six olefinic carbons [δ_C 124.0 (C-4), 162.8 (C-5), 126.4 (C-6), 133.4 (C-7), 129.7 (C-8), and 151.6 (C-14)], and a carbonyl group [δ_C 199.3 (C-3)]} and side chain {four methyl groups [δ_H 1.12 (d, J = 7.2, H-21), 1.00 (d, J = 7.2, H-28), 1.18 (s, H-27), and 1.15 (s, H-26)], two methines [δ_H 2.89 (t-like, J = 9.0, H-20) and 2.17 (m, H-24)], two olefinic carbons [δ_C 136.7 (C-22) and 131.1 (C-23)], and a quaternary carbon with oxygen function group [δ_C 72.4 (C-25)]} with methoxy group [δ_H 3.37 (C-15-OMe)]. In addition, ^{1}H and ^{13}C NMR spectra of **1** were similar to those of 15β-methoxy-ergosta-4,6,8(14),22-tetraen-3-one[18] except for the signals from C-11, 12, 13, 24, 25, 26, and 27. Above analysis suggested that **1** is the ergosterol derivative having two more hydroxy group than 15β-methoxy-ergosta-4,6,8(14),22-tetraen-3-one. The HMBC correlations of H-18/C-12, H-18/C-13, H-18/C-14, H-18/C-17, H-C15-O*Me*/C-15, H-27/C-25, H-27/C-24, and H-27/C-26 suggested that two hydroxy groups and methoxy located at C-12, C-25, and C-15, respectively

(Figure 2). The relative stereo structure on 6/6/6/5 ring system were determined by NOESY spectra. NOESY cross-peaks corresponding to H-18/H-11*β*, H-11*β*/H-19, and H-18/H-21 suggested that H-11*β*, C-18, C-19, and sidechain including C-21 were located at same side. Also, NOESY cross-peaks corresponding to H-9/H-12, H-12/H-17, and H-15/H-17 suggested that H-9, H-12, H-15, and H-17 were located at same side (Figure 2). The suggested relative stereo chemistry on the 6/6/6/5 ring system was identical with that of ergostane-type steroids isolated from *A. terreus*.[18] In addition to the above analysis and the chemical structures of known ergostane-type steroids produced by fungi,[19] we deduced the relative stereo chemistry including side chain were deduced as 9*R**,10*R**,12*R**,13*R**,15*R**,17*R**, 20*R**, 24*S**. According to the positive optical rotation, we deduced the absolute stereochemistry was same as 15*β*-methoxy-ergosta-4,6,8(14),22-tetraen-3-one ($[a]^{20.4}_{D}$ +231.8 in methanol).[19] Based on the evidence, the chemical structure of terreus steroid (**1**) was established as shown in Figure 1.

Table 1. ^{13}C (150 MHz) and ^{1}H (600 MHz) NMR data of terreus steroid (**1**) in chroloform-*d*

position	δ_C	δ_H (*J* in Hz)
1	34.0	*α* 1.83 (m) *β* 1.98 (m)
2	33.9	2.51 (m)
3	199.3	
4	124.0	5.76 (s)
5	162.8	
6	126.4	6.10 (d, 9.6)
7	133.4	6.90 (d, 9.6)
8	129.7	
9	45.2	2.49 (m)
10	36.8	
11	28.6	*α* 1.76 (m) *β* 1.67 (m)
12	75.8	3.76 (dd, 4.2, 11.4)
13	48.9	
14	151.6	
15	78.6	4.44 (d-like, 3.6)
16	29.6	*α* 1.82 (m) *β* 1.90 (m)
17	53.7	1.82 (m)
18	15.7	0.93 (s)
19	17.0	1.04 (s)
20	36.5	2.89 (t-like, 9.0)
21	23.0	1.12 (d, 7.2)
22	136.7	5.52 (dd, 9.0, 15.6)
23	131.1	5.37 (dd, 8.4, 15.6)
24	48.5	2.17 (m)
25	72.4	
26	26.5	1.15 (s)
27	27.0	1.18 (s)
28	15.5	1.00 (d, 7.2)
15-OMe	56.6	3.37 (s)

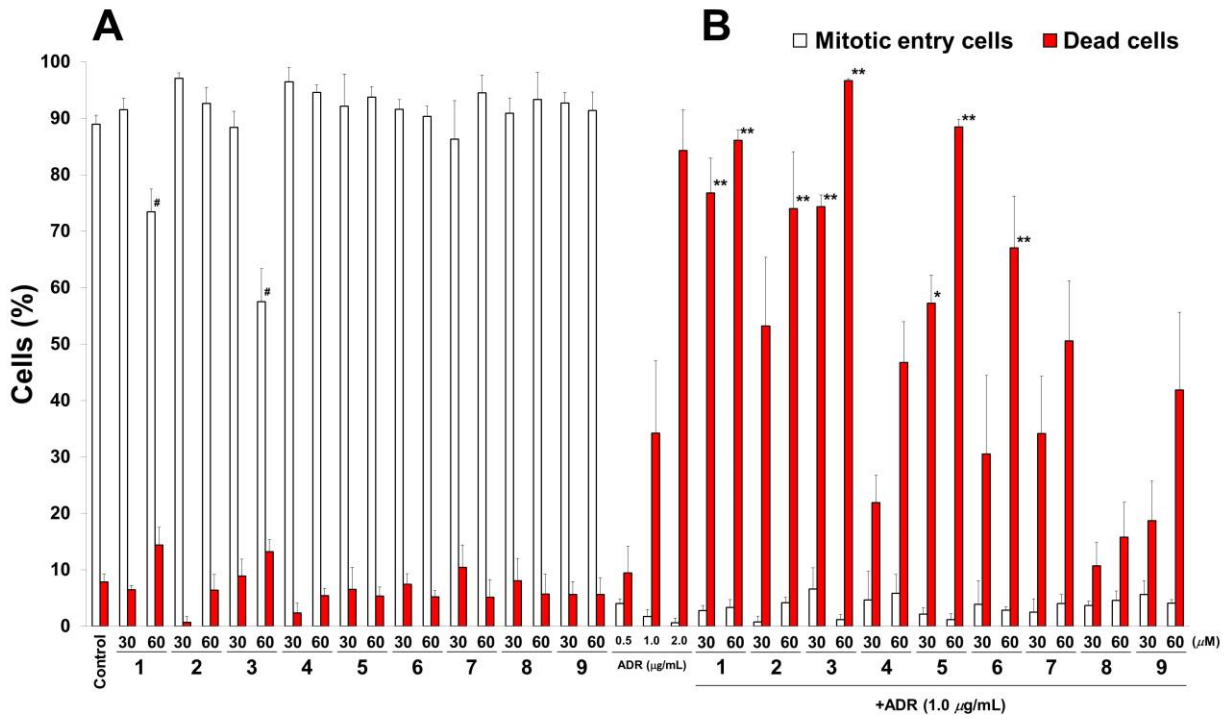

Figure 3. The effects of isolated compounds (**1**–**9**) and ADR on cell proliferation and cell death. The number of mitotic entry cells (*white columns*) and dead cells (*red columns*) were counted using a time-lapse recording. The graph shows the percentages of mitotic entry cells and dead cells as the means ± S.D. of three independent experiments. Statistical significance was analyzed using the Tukey-Kramer test. (A) HeLa cells were treated with 30 or 60 μM of isolated compounds (**1**–**9**) or 0.5, 1.0, and 2.0 μg/mL of ADR for 24 h. $^{\#}p < 0.001$ compared with control group. (B) HeLa cells were treated with 30 or 60 μM of isolated compounds (**1**–**9**) in combination with ADR (1.0 μg/mL). $^{*}p < 0.05$ and $^{**}p < 0.001$ compared with ADR (1.0 μg/mL) group.

ADR is frequently used for cancer therapy for its broad-spectrum effects. ADR inhibits cell proliferation through the induction of G2/M cell cycle arrest via DNA damage. However, its benefit is limited by a series of side effects such as induction of apoptosis on cardiomyocytes and over production of reactive oxygen species.[20] The drug efflux function of P-gp and anti-apoptotic function of heat shock protein (HSP) are well-known elements that decrease the sensitivity of cancer cells to ADR. Therefore, inhibitors of P-gp and HSP may be able to reduce ADR dosage in tumor therapy to preventing side effects. Previously, we reported the inhibitors of P-gp activity[21] and HSP expression[22] induce cell death on ADR-treated HeLa cells. In this study, we evaluated the cell death inducing activity of isolated compounds (**1**−**9**) on ADR-treated HeLa cells using time-lapse cell imaging analysis. In this assay, we counted the number of mitotic entry cells and dead cells treated with ADR (0.5, 1.0, or 2.0 μg/mL), isolated compounds (**1**−**9**, 30 or 60 μM), and isolated compounds (**1**−**9**, 30 or 60 μM) with ADR (1.0

μg/mL). The isolated compounds **1** and **3** significantly decreased the number of mitotic entry cells and weakly increased dead cells at 60 μM. Compounds **2** and **4**–**9** didn't affect the number of mitotic entry cells and dead cells (Figure 3A). The number of dead cells induced by ADR was significantly increased by the compounds **1**−**3**, **5**, and **6** (Figure 3B). Namely, compounds **2**, **5**, and **6** enhanced the cell death inducing activity of ADR, however, they didn't show anti-proliferative effects without ADR. Moreover, the number of dead cells with combination treatment of **1**, **3**, and **5** (60 μM) with ADR (1.0 μg/mL) were larger than that of 2.0 μg/mL ADR treated cells. According to these results, **1**−**3**, **5**, and **6**, especially **5** may have a potential to enhance the effects of cancer treatment agents such as ADR.

EXPERIMENTAL

Specific rotations were obtained by using a JASCO P-2200 digital polarimeter (l = 5 cm). FABMS and HRFABMS were recorded by using a JEOL JMS-SX102A mass spectrometer. UV spectra were measured on a model J-1500 spectrometer (JASCO). FTIR spectra were recorded on a model FT/IR-4600 Fourier transform infrared spectrometer (JASCO). ^{1}H NMR spectroscopy was recorded on JEOL ECS400 (400 MHz) and JNM-ECA 600 (600 MHz) spectrometers. ^{13}C NMR spectroscopy was recorded on a JNM-ECA 600 (150 MHz) spectrometer. 2D-NMR experiments were carried out on a JEOL JNM-ECA 600 (600 MHz) spectrometer. Normal phase silica gel column chromatography was carried out using Silica gel 60 (Kanto Chemical Co., Inc. 63–210 mesh), and reversed phase silica gel column chromatography was carried out using C_{18}-OPN (Nacalai Tesque Co., Inc. 140 μm). Thin-layer chromatography (TLC) analysis was carried out using precoated TLC plates with Silica gel 60F_{254} (Merck, 0.25 mm) (ordinary phase) and Silica gel RP-18 F_{254S} (Merck, 0.25 mm) (reversed phase). Detection was achieved by spraying with 1% $Ce(SO_4)_2$–10% aqueous H_2SO_4 followed by heating. High-performance liquid chromatography (HPLC) was performed using a Shimadzu SPD-M20A UV–vis detector, Shimadzu LC-20AD pump, and Shimadzu SIL-20A auto-injector. COSMOSIL 5C_{18}-MS-II (Nacalai Tesque Co., Inc. 250 × 4.6 mm i.d., 250 × 10 mm i.d., and 250 × 20 mm i.d.) columns were used for analytical and preparative work.

Collection and identification of the JKYM-KI3 strain. Airborne particles (PM_{10}, aerodynamic diameter ≤ 10 μm) were collected in the city of Kyoto (135.81°E, 34.99°N) using a high-volume air sampler (HV1000R, Shibata Scientific Technology, Soka) equipped with an impactor (Shibata Scientific Technology) in March 2022. The collected airborne particles were immediately suspended in distilled H_2O. The suspension was inoculated with potato dextrose agar (PDA) and chloramphenicol (0.1 g/L) for incubating at 27 °C for 3 days. The JKYM-KI3 strain was isolated as colonies and stored in 10% glycerin at −80 °C. Using internal transcribed spacer 1 (ITS1, 5′-TCCGTAGGTGAACCTGCGG-3′) and ITS4 (5′-TCCTCCGCTTATTGATATGC-3′) as primers, the ITS1-5.8S-ITS2 sequence region (364 base pairs,

GenBank accession number OQ186858) of JKYM-KI3 was obtained. BLAST analysis (NCBI database) showed that the sequence has a 99.73% identity of *Aspergillus terreus* (Accession number: MT558939).

Fermentation and extraction. The seed culture of the fungus was prepared in a potato dextrose medium and incubated at 27 °C for 5 days at 200 rpm. The seed cultures were added to 1000 of 90 mm Petri dishes containing PDA. The cultures were milled by liquidizer (MJA-G100, Yamazen, Osaka) after incubation at 27 °C for 14 days. The milled cultures were added H_2O and partitioned with EtOAc.

Isolation of the compounds produced by the *A. terreus* JKYM-KI3 strain. The EtOAc soluble fraction (54.5 g) was purified by normal phase silica gel column chromatography [*n*-hexane–$CHCl_3$ (1:1 → 1:5→ 0:1, v/v) → $CHCl_3$–MeOH (50:1 → 30:1 → 10:1 → 5:1 → 3:1 → 1:1 → 0:1, v/v)]. TLC analysis was used for visualization of the constituents for fractionation. Thus, the nine fractions (Fraction 1–9) were collected. Fraction 3 (5.5 g) was further separated using reversed phase silica gel column chromatography [MeCN–H_2O (2:8 → 1:0, v/v)] and nine fractions were collected. Fraction 3-3 (143.6 mg) was purified using HPLC [MeCN–H_2O (40:60, v/v)] to obtain **4** (80.0 mg). Fraction 3-4 (303.9 mg) was purified using HPLC [MeCN–H_2O (40:60, v/v)] to obtain **2** (23.1 mg), **5** (32.5 mg), and **6** (81.3 mg). Fraction 3-6 (360.9 mg) was purified using HPLC [H_2O–MeCN (55:45, v/v)] to obtain **3** (19.1 mg). Fraction 4 (11.0 g) was separated using reversed phase silica gel column chromatography [MeCN–H_2O (1:9 → 1:0, v/v)] and eight fractions were obtained. Fraction 4-4 (4.5 g) was purified using HPLC {MeCN–H_2O (45:55, v/v)} to obtain **7** (106.2 mg), **8** (11.7 mg), and **9** (10.4 mg). Fraction 4-5 (2.2 g) was purified using HPLC [MeCN–H_2O (50:50, v/v)] to obtain **1** (1.9 mg).

Terreus steroid (1): Colorless amorphous powder; $[\alpha]^{25}_{D}$ +201.9 (*c* 0.1, MeOH); UV (MeOH) λ_{max} 197.6 nm (log ε 4.1), 341.1 nm (log ε 4.00), IR (ATR) ν_{max} 2966, 1647, 1587, 1457, 1414, 1375, 1072, 1033 cm^{-1}; ^1H NMR (chroloform-*d*, 600 MHz) and ^{13}C NMR (chroloform-*d*, 150 MHz) see Table 1; FABMS: *m/z* 455 $[M+H]^+$; HRFABMS: *m/z* 455.3179 (Calcd for $C_{29}H_{43}O_4$ $[M+H]^+$: *m/z* 455.3161).

Time-lapse imaging analysis. Time-lapse imaging was performed on an Operetta high-content imaging system (PerkinElmer, Waltham, MA, USA). HeLa cells were cultured in a flat-bottomed 96-well plate (Coster 3596; Corning, NY, USA) and incubated to reach 70−80% confluence. The cells were treated with the test compounds prior to the time-lapse cell imaging. The images were captured at 10 min intervals for 24 h under a 5% CO_2 atmosphere at 37 °C. Based on these images, the number of mitotic cells and dead cells within 24 h was quantified.

Statistical Analysis. Statistical analyses were conducted using GraphPad Prism 8.43 software. The statistical analysis was conducted using one-way analysis of variance (ANOVA) followed by a Tukey-Kramer test to analyze the differences between the treatment groups.

SUPPORTING INFORMATION

Experimental details: 1D and 2D-NMR spectra for terreus steroid (**1**) are available free of charge on the Internet.

ACKNOWLEDGEMENTS

This work was supported by JSPS KAKENHI Grant Numbers 20H03397.

REFERENCES

1. C. Qi, M. Liu, Q. Zhou, W. Gao, C. Chen, Y, Lai, Z. Hu, Y. Xue, J. Zhang, A. Li, X. N. Li, Q. Zhang, J. Wang, H. Zhu, and Y. Zhang, *J. Nat. Prod.*, 2018, **81**, 1937.
2. K. A. U. Zaman, Z. Hu, X. Wu, S. Hou, J. Saito, T. P. Kondratyuk, J. M. Pezzuto, and S. Cao, *J. Nat. Prod.*, 2020, **83**, 730.
3. F. He, J. Bao, X. Y. Zhang, Z. C. Tu, Y. M. Shi, and S. H. Qi, *J. Nat. Prod.*, 2013, **76**, 1182.
4. W. Ebrahim, M. E. Neketi, L. I. Lewald, R. S. Orfali, W. Lin, N. Rehberg, R. Kalscheuer, G. Daletos, and P. Proksch. *J. Nat. Prod.*, 2016, **79**, 914.
5. J. Bao, X. X. Li, K. Zhu, F. He, Y. Y. Wang, J. H. Yu, X. Zhang, and H, Zhang, *Fitoterapia*, 2021, **150**, 104856.
6. J. Wei, X. Chen, Y. Ge, Q. Yin, Y. Ma, Z. Zhang, X. Wu, K. Hong, and B. Wu, *Phytochemistry*, 2023, **205**, 113479.
7. Z. Wu, D. Li, F. Zeng, Q. Tong, Y. Zheng, J. Liu, Q. Zhou, X. N. Li, C. Chen, Y. Lai, H. Zhu, and Y. Zhang, *Phytochemistry*, 2018, **156**, 159.
8. T. Matsumoto, T. Kitagawa, D. Imahori, A. Matsuzaki, Y. Saito, T. Ohta, T. Yoshida, Y. Nakayama, E. Ashihara, and T. Watanabe, *Bioorg. Med. Chem.*, 2021, **45**, 128161.
9. T. Matsumoto, D. Imahori, Y. Saito, W. Zhang, T. Ohta, T. Yoshida, Y. Nakayama, E. Ashihara, and T. Watanabe, *J. Nat. Med.*, 2020, **74**, 689.
10. T. Matsumoto, D. Imahori, E. Ohnishi, M. Okayama, T. Kitagawa, T. Ohta, T. Yoshida, N. Kojima, M. Yamashita, and T. Watanabe, *Fitoterapia*, 2022, **156**, 105097.
11. X. H. Nong, Y. F. Wanf, X. Y. Zhang, M. P. Zhou, X. Y. Xu, and S. H. Qi, *Mar. Drugs*, 2014, **12**, 6113.
12. F. C. Peng, *J. Nat. Prod.*, 1997, **60**, 842.
13. G. Y. Li, B. G. Li, T. Yang, J. H. Yin, H. Y. Qi, G. Y. Li, and G. L. Zhang, *J. Nat. Prod.*, 2005, **68**, 1243.
14. C. Rank, R. K. Phipps, P. Harris, J. C. Frisvad, C. H. Gotfredsen, and T. O. Larsen, *Tetrahedron Lett.*, 2006, **47**, 6099.

15. J. R. Chavez, D. C. Blancas, and J. M. Jimenez, *Bioorg. Med. Chem.*, 2020, **28**, 115817.
16. M. You, L. Liao, S. H. Hong, W. Park, D. I. Kwon, J. Lee, M. Noh, D. C. Oh, K. B. Oh, and J. Shin, *Mar. Drugs*, 2015, **13**, 1290.
17. G. Y. Chen, B. H. Ruan, Y. B. Yang, Q. Wang, X. Z. Li, N. Luo, X. Q. Yang, and L. X. Zhao, *Chem. Nat. Compd.*, 2018, **54**, 415.
18. R. Haritakun, P. Rachtawee, S. Komwijit, S. Nithithanasilp, and M. Isaka, *Helv. Chim. Acta*, 2012, **95**, 308.
19. S. Wang, L. Zhang, L. Y. Liu, Z. J. Dong, Z. H. Li, and J. K. Liu, *Nat. Prod. Bioprospect.*, 2012, **2**, 240.
20. J. Zhang, Y. Zha, Y. Jiao, Y. Li, and S. Zhang, *Toxicology*, 2023, **485**, 153426.
21. D. Imahori, T. Matsumoto, Y. Saito, T. Ohta, T. Yoshida, Y. Nakayama, and T. Watanabe, *Fitoterapia*, 2021, **154**, 105023.
22. T. Matsumoto, T. Kitagawa, D. Imahori, H. Yoshikawa, M. Okayama, M. Kobayashi, N. Kojima, M. Yamashita, and T. Watanabe, *J. Nat. Med.*, 2021, **75**, 942.